We are IntechOpen, the world's leading publisher of Open Access books Built by scientists, for scientists

6,900
Open access books available

185,000
International authors and editors

200M
Downloads

Our authors are among the

154
Countries delivered to

TOP 1%
most cited scientists

12.2%
Contributors from top 500 universities



WEB OF SCIENCE™

Selection of our books indexed in the Book Citation Index in Web of Science™ Core Collection (BKCI)

Interested in publishing with us?
Contact book.department@intechopen.com

Numbers displayed above are based on latest data collected.
For more information visit www.intechopen.com



Chapter

Convective Drying in the Multistage Shelf Dryers: Theoretical Bases and Practical Implementation

Artem Artyukhov, Nadiia Artyukhova, Ruslan Ostroha, Mykola Yukhymenko, Jozef Bocko and Jan Krmela

Abstract

The main advantages regarding the convective drying of the granular materials in the multistage dryers with sloping perforated shelves were represented. Peculiarities of the shelf dryers' hydrodynamics were shown in the research. Various hydrodynamic weighing modes were experimentally justified, and the relevant criteria equations were obtained. The results of investigations regarding the interphase heat and mass transfer were given; criteria dependencies, which predict heat and mass transfer coefficients in the shelf dryers, were proposed. A method to assess the efficiency of the dehydration process at the separate stages of the device and in the dryer, in general, was proposed. The algorithm to define the residence time of the granular material on the perforated shelf with a description of the author's software product for optimization calculation was shown. The shelf dryers' engineering calculation method was presented in this work. The original constructions of devices with various ways to control the residence time of the granular material that stays in their workspace were described. The testing results of the shelf dryer to dry granular materials, such as coarse- and fine-crystalline potassium chloride, sodium pyrosulfate, and iron and nickel powders, were demonstrated.

Keywords: convective drying, multistage shelf dryer, hydrodynamics, interphase heat and mass transfer, efficiency of dehydration, engineering calculation, industrial implementation

1. Introduction

Convective drying is one of the most effective methods for disperse material dehydration in the chemical, pharmaceutical, mining, and other industrial branches [1–6]. The direct contact of the drying agent with high-temperature potential and dried material enables intensively to remove the surface and adsorption-bound moisture [3]. That is why drying is the only method for industries to achieve the required quality of the product.

Although during drying the energy consumption is the lowest, the convective dryers are more often used to dry disperse materials thanks to other numerous

advantages [3, 4]. Provision of the active hydrodynamic regime in such dryers helps intensify the process without reduction of the economic efficiency of their operation and has the following advantages [7–9]:

- Hydrodynamic stability of the process
- Increase of the relative motion velocity of the interacting phases
- The developed surface of the contacting phases
- Approximation of the hydrodynamic model of flows in the device to the ideal displacement model
- Reduction of the energy intensity of the process and metal intensity of devices

One should distinguish devices with various configurations of the weighted layer (fluidized bed, spouting, gravitational falling, vortex, etc.,) from the variety of the convective dryer constructions (described, e.g., in [7, 10]). Thanks to the developed surface of the phase contact, devices with hydrodynamic system are characterized with high intensity of the heat and mass transfer processes, lower non-energy costs, and have high specific productivity [7].

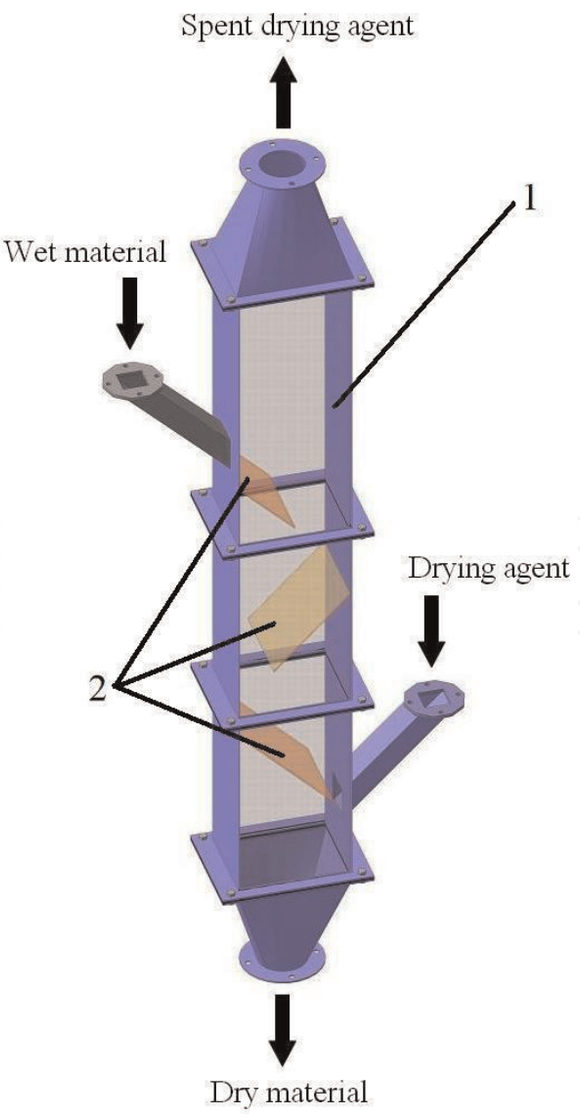


Figure 1.
Multistage shelf dryer: (1) case; (2) shelf.

Besides, under conditions of the cost increase to prepare and to transport the drying agent, the possibility of its repeated use in the drying process is fundamentally important. Therefore it is necessary maximum to use the thermal potential of the drying agent during every contact with disperse material. It can be achieved while using the multistage drying devices with vertical sectioning of the workspace by the perforated shelf elements [7, 8, 11].

A solution to the permanent residence of the dispersed material in the "active" zone can be found through implementation of the multistage shelf dryers with vertical sectioning of the workspace (**Figure 1**).

In such devices, the conditions for the differentiated heat treatment of materials can be created owing to the drying agent potential and peculiarities of each stage (shelf) construction. So, moving the perforated shelf to the wall of the device, we approach to the device with fluidized bed, and moving it away from the wall and freeing its workspace, we approach to the device with the free intersection, such as pneumatic transportation dryers. The shelves increase the residence time of the dried material particles, either poured downward of the device or carried out upward of it. The shelves increase the velocity and turbulence of the gas flow, create a vortex motion in their location places, and increase the contact intensity between phases. The free space between the ends of the shelves and the walls of the device does not require special flows from the upper shelf to the lower one. Changing the free area of the shelve perforation, their tilt angles, the distance from the end of the shelves to the walls of the device, the number of shelves, and the distance between them vertically, it is possible to influence the intensity of the contact phases and to create different hydrodynamic regimes to weigh particles of the material both on individual shelves and heightwise the device. Therefore, it is possible to carry out the drying process of wet materials and its pneumatic classification in one device in order to remove small dusty fractions from the mixture [7].

2. Theoretical basics

The necessity to determine these features is due to the fact that before constructing an industrial sample of the gravitational shelf dryer it is necessary to determine its optimal design. In this case, the optimization criterion is to ensure the minimum required residence time of the dispersed phase in the working space of the dryer, which will complete the drying process to a predetermined humidity indicator. It is important to observe the condition, under which the "hydrodynamic" residence time of the dispersed phase in the workspace of the device should be no less than the "thermodynamic" time (this parameter is determined by the kinetics of the moisture removal process from the dispersed phase). Therefore, in order to keep the integrity of the dispersed particles, the "hydrodynamic" time should not exceed the "thermodynamic" time by more than 5–10%. By adjusting the hydrodynamic properties of the flow, an optimal construction of the gravitational shelf dryer is achieved, which meets the requirements of the optimization criterion.

Thus, the optimization calculation of the dryer consists of three blocks: hydrodynamic calculation (calculation of the residence time of a particle on a stage), kinetic calculation (kinetic parameter of the moisture removal), and calculation of drying efficiency.

Initial data (**Figure 2**):

- Rate of gas flow, Q (m^3/s)
- Length of device, L (m)

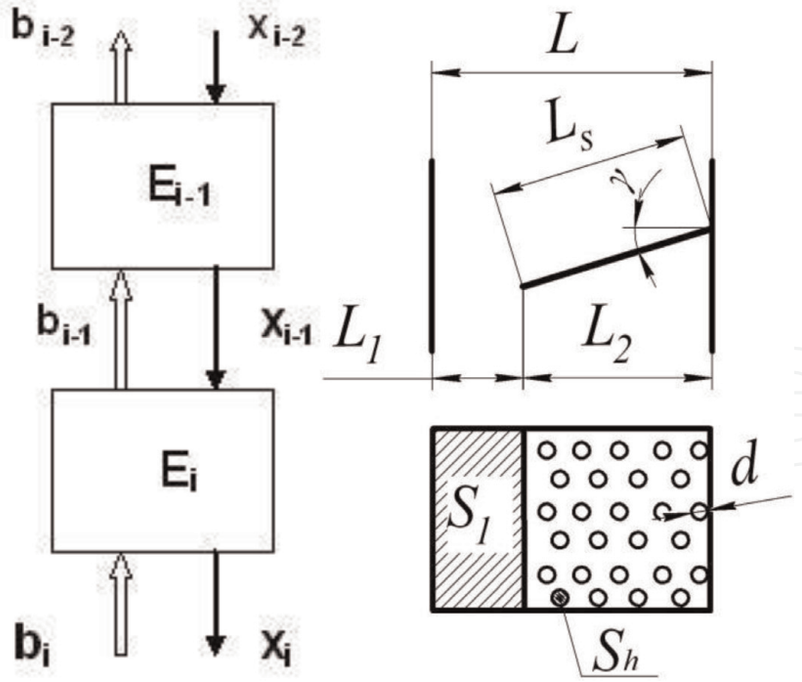


Figure 2.
A fragment of the calculation scheme for the multistage drying: left figure—change of flows' moisture: x, moisture of the disperse material; b, moisture of the drying agent, and right figure—construction of dryer's workspace.

- Overall width of device, h (m)
- Length of shelf, L_s (m)
- Degree of perforation (free area), δ
- Perforation hole diameter, d (m)
- The tilt angle of shelf, γ (°)
- The radius of the granule, r_{gr} (m)
- Granule density, ρ_{gr} (kg/m^3)
- Gas density, ρ_g (kg/m^3)
- Acceleration of gravity, g (m/s^2)
- Resistance coefficient, ξ
- Volumetric content of a dispersed phase in a two-phase flow, ψ
- The coefficient that takes into account the tightness of the flow, m
- Number of stages in dryer, i
- Moisture of the material i-stage of the dryer x (kg of water/kg of material)
- Moisture of the drying agent in i-stage of the dryer b (kg of water/kg of material)

2.1 Hydrodynamic calculation

Hole area on the shelf (horizontal position) (m^2)

$$S_h = \frac{\pi d^2}{4}. \tag{1}$$

The perforated area on the shelf (horizontal position of the shelf) (m^2)

$$\sum S_h = L_s \cdot h \cdot \delta. \tag{2}$$

Number of holes on the shelf

$$n = \frac{\sum S_h}{S_h}. \tag{3}$$

Area of outloading clearance (m^2)

$$S_1 = (L - L_s \cos\gamma) \cdot h. \tag{4}$$

Area of the gas passage holes in the shelf (inclined position of the shelf) (m^2)

$$S_2 = \frac{\pi d^2}{4} \cdot n \cdot \cos\gamma. \tag{5}$$

The relative area of outloading clearance

$$S_1^r = \frac{S_1}{S_1 + S_2}. \tag{6}$$

The relative area of the gas passage holes in the shelf

$$S_2^r = \frac{S_2}{S_1 + S_2}. \tag{7}$$

Rate of the gas flow in outloading clearance (m^3/s)

$$Q_1 = Q \cdot S_1^r. \tag{8}$$

Rate of the gas flow in holes in the shelf (m^3/s)

$$Q_2 = Q \cdot S_2^r. \tag{9}$$

Gas velocity in holes in the shelf (m/s)

$$V_{work} = {}^{Q_2}\!/_{S_2}. \tag{10}$$

Second critical velocity (m/s)

$$V_{cr} = 1.63 \cdot \sqrt{\frac{\rho_{dr} \cdot g \cdot r_{gr}}{\xi \cdot \rho_g}}. \tag{11}$$

Velocity difference (m/s)

$$\Delta V = V_{cr} - V_{work}. \tag{12}$$

Time of material residence on the shelf (free movement) (s)

$$\tau_f = \frac{L_s}{\Delta V \sin \gamma}. \tag{13}$$

The empirical function of the effect of compression on the residence time of the particle in the working space of the device

$$f_{e\tau}(\psi) = (1-\psi)^{-m}. \tag{14}$$

Time of material residence on the shelf (straitened movement) (s)

$$\tau_s = \frac{L_s \cdot f_{e\tau}(\psi)}{\Delta V \sin \gamma}. \tag{15}$$

The program Multistage Fluidizer® [12] used Hypertext Markup Language HTML, Cascading Style Sheet (CSS), and programing language JavaScript (including the library jQuery). HTML is presented as a tagging of web-based app, CSS page formatting. JavaScript is used to calculate and transfer data and to create animation and data validation effect. In the validation block of JavaScript, data accuracy is checked. In the block input info, the basic data field indices are accepted, and they are written to the object of input_information. In the block, calculation computations are carried out by Eqs. (1)–(15).

Index.html (**Figure 3**) is the main page of the web-based app. It is responsible for reflection of the main menu, for the main calculation of gas flow, and for jumping the other pages (an example of such page is presented in **Figure 4**), where the main dependencies between key features to calculate gas flow and resistance time of the material on the shelf are calculated and dependencies diagrams are formed.

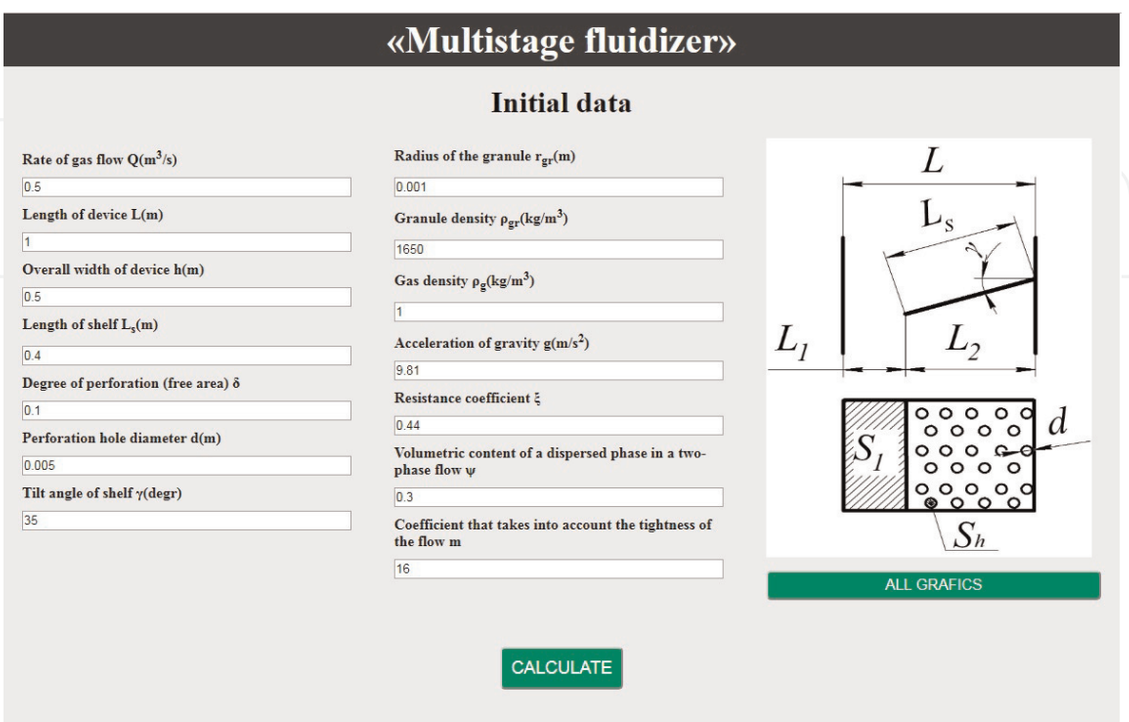


Figure 3.
The main page of the Multistage Fluidizer® software.

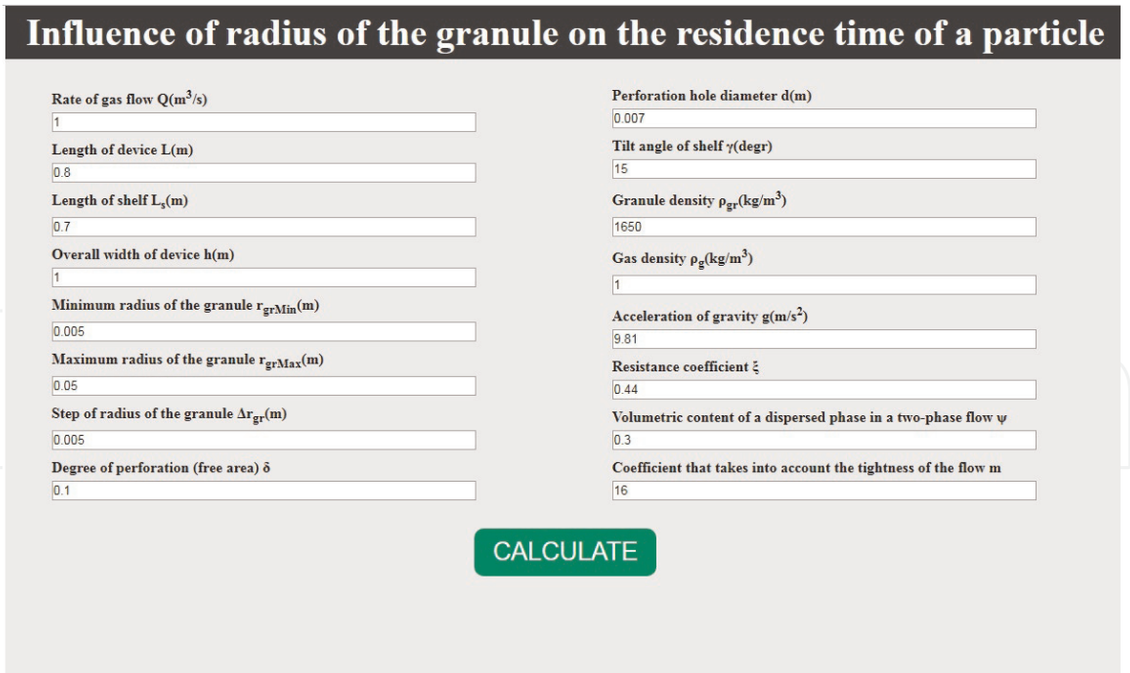


Figure 4.
Calculation page of various parameter impacts on the particle resistance time in the device.

Having inserted data, data validity is tested, that is, if all data is correct, after keystroke CALCULATE data is processed given the above formulas, and we receive the result in a form of a computation table (**Figure 5**).

After changes of indices l_f and l_s, it is possible to see how the animation appears after the pressing the "Show calculation" button (the example of distance length calculation, which particle takes on the shelf during the specified period of time, is shown in **Figure 6**). In order to create animation, functions clicker_lf and clicker_ls are implemented, respectively, for τ_f and τ_s animation.

In JavaScript, one uses libraries jQuery and table2excel, objects for data recording, methods .val() .append() to read and to insert indices to fields, methods

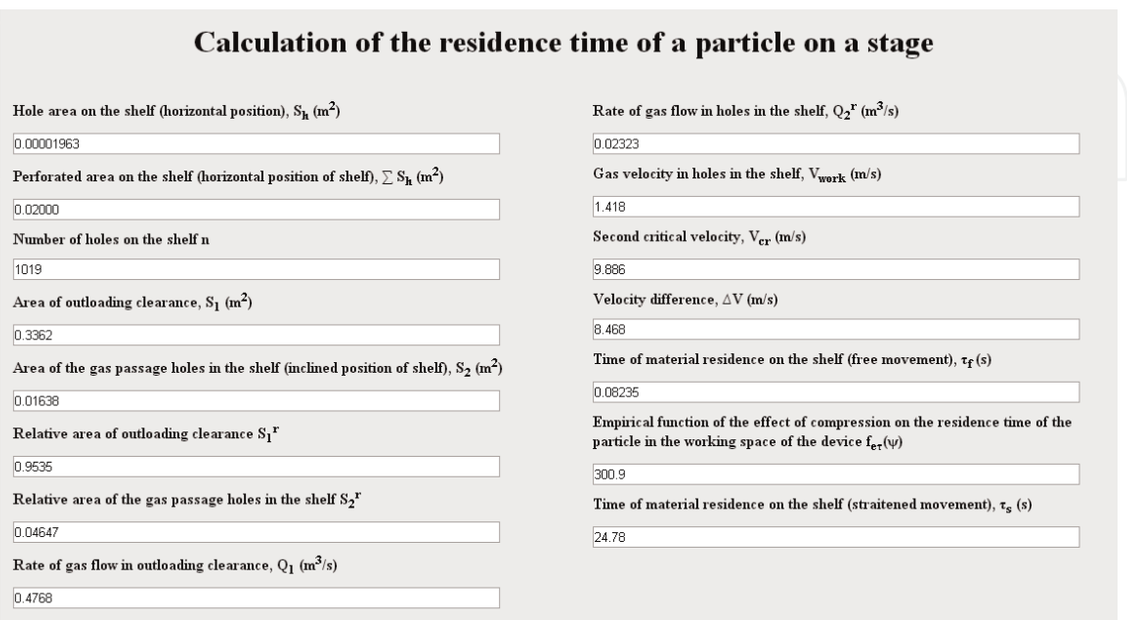


Figure 5.
Results of calculation.

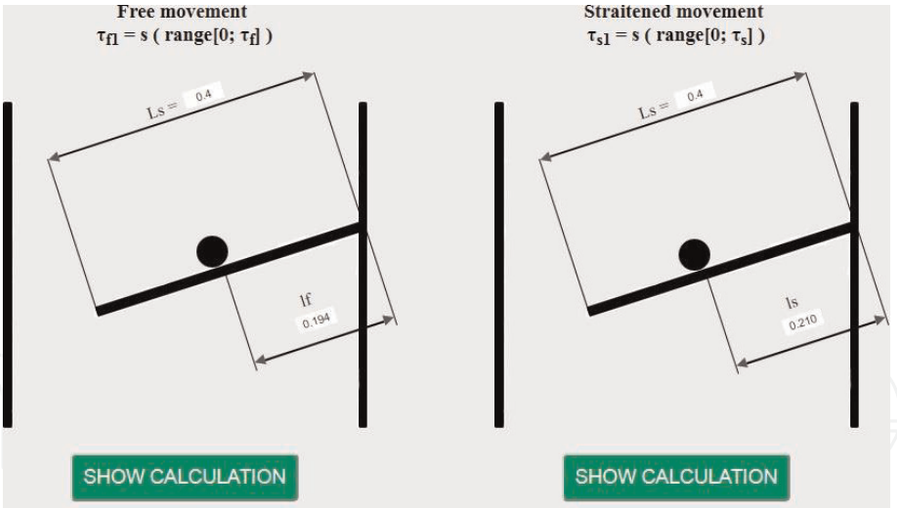


Figure 6.
Calculation of way length, which particle undergoes on the shelf during the specified period of time.

.removeClass() and .addClass() to delete and to add classes, and method .animate() for work with animation to create an animation effect for any digital CSS feature of the element.

2.2 Calculation of heat-mass transfer

In order to calculate the kinetic parameter of the moisture removal (the moisture-yielding capacity coefficient), let us use the following algorithm.

It is proposed [8] to use the following equation for calculation of β:

$$\frac{\Delta U_m}{\tau} = \beta \cdot F \cdot \left(b_{fin} - \frac{b_{fin} + b_{in}}{2} \right) \cdot \rho_g, \tag{16}$$

where b_{in}, b_{fin}, and ΔU_m are the initial and final humidity of the drying agent and the amount of the removed moisture from the material; F is the surface of the mass transfer, which depends on the dryer's effective operation due to the disperse material and the residence time of the material in the dryer.

In general, the criteria equation of the drying process can be written as follows:

$$Sh = A_1 \cdot Sc^n \cdot \mathrm{Re}^m, \tag{17}$$

where A_1 is the equation coefficient; $Sh = \frac{\beta \cdot d_{gre}}{D}$ is the Sherwood criterion; d_{gre} is the equivalent diameter of the particle (granule), m; $Sc = \frac{\nu}{D}$ is the Schmidt criterion; $\mathrm{Re} = \frac{V_{work} \cdot d_{gre}}{\nu}$ is the Reynolds criterion; D is the diffusion coefficient of the gas flow, m^2/s; ν is the kinematic viscosity coefficient of the gas flow, m^2/s; and m and n are the indicators of the equation stages, which are evaluated through the graphical dependency $Sh/Sc^{0.33} = f(Re)$, obtained from the experimental data.

2.3 Calculation of the kinetics and drying efficiency

The drying process effectiveness on the i-stage of the dryer is presented by the ratio of differences between the moisture contents of the disperse material before and after the drying $x_{i-1} - x_i$ to the maximum possible (theoretical) difference between the moisture contents on the stage $x_{i-1} - b_i$ and also in the form of the function of the kinetic parameter of the moisture transfer B_i, the residence time of

the material on the stage τ_i, and the consumption ratio of the dispersed phase to the drying agent G_i^{-1} [8]:

$$E_i = \frac{\Delta x}{\Delta x_{\max}} = \frac{x_{i-1} - x_i}{x_{i-1} - b_i} = \frac{1 - \exp\left[-\beta_i \tau_i \left(1 + G_i^{-1}\right)\right]}{1 + G_i^{-1}}. \tag{18}$$

3. Visualization of results and discussion

3.1 Hydrodynamics

Some graphic dependencies are shown in **Figure 7**. The program receives two- and three-dimensional dependency graphs.

In general dependency diagrams, features for free and constraint motion of particles have one functional dependence. The particle resistance time has enough narrow diapason at every stage (shelf) in free motion regime and is calculated by second units. In the constraint motion regime of particles, the residence time is greatly increased at every stage. The abundant ratio of particles in the two-phase system has a definite impact on this index. That is why, while defining the optimum performance of the device, it is necessary to define the workspace size of the granulating or drying device to high accuracy.

The impact made by some constructive features of the shelf dryer during the residence time of the dispersed material (**Figure 7**) is shown below.

The change of the shelf tilt angle to the horizon affects the redistribution of the gravity components: enlargement of it leads to an increase of the gravity rolling component and vice versa. It should be mentioned that the tilt angle of the shelf may have a minimum value that complies with the natural slope angle of the material. As the tilt angle of the shelf decreases, the residence time of the dispersed material gradually increases. It leads to longer contact with the drying agent's flow.

Changing the gap between the edge of the shelf and the dryer's wall significantly influences the change of the residence time of the dispersed material on the shelf. If the gap increases, the contact time of the dispersed material with the drying agent will be reduced due to the decrease in the length of the material movement distance on the shelf. In this case, the operation of the rolling component of the dispersed material velocity lasts for a shorter period and at the end of the shelf is replaced by the full gravity. Thus, the material moves down, and only the ascending gas flow force resists its fall.

The analysis of the calculations regarding the effect, made by the free cross-sectional area of the shelf on the drying process efficiency, showed the following. Reducing the free cross-sectional area of the shelf leads to an increase of the drying agent's ascending motion velocity in the holes. In this case, the action of the drying agent's ascending flow slows down the progressive motion of the dispersed material on the shelf, compensating for the rolling component of its gravity. The pulse component of the dispersed material displacement decreases, and the trajectory changes to a pulse-forward one. The trajectory length of the dispersed material motion increases, the time of its contact with the drying agent is extended.

As the diameter of the perforation holes decreases, the effect of the drying agent's ascending flow increases, in which the pulse component of the dispersed material motion trajectory decreases, and the forward increases. Thus, the trajectory length of the dispersed material motion increases, and the contact time with the drying agent is extended. It should be noted that with the further reduction of the perforation hole diameter, the action of the drying agent's ascending flow begins

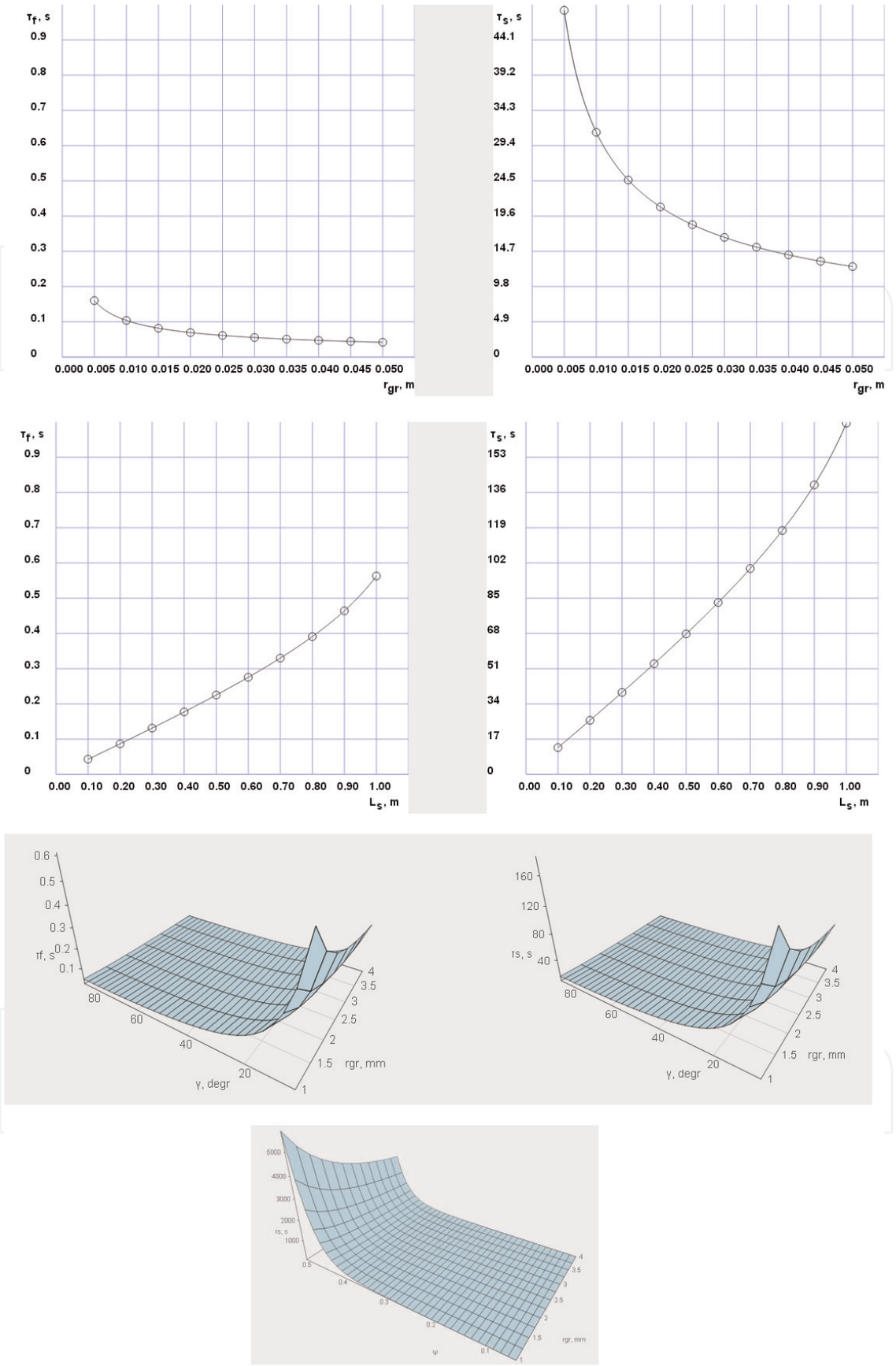


Figure 7.
Examples of calculation results.

significantly to outweigh the effect of the gravity rolling component. It leads to the formation of the second transitional mode and the ablation mode in the shelf dryer's operation.

3.2 Heat-mass transfer

The calculated values of the mass transfer coefficient β from Eq. (16) depending on the velocity of the drying agent's motion are demonstrated in **Figure 8**.

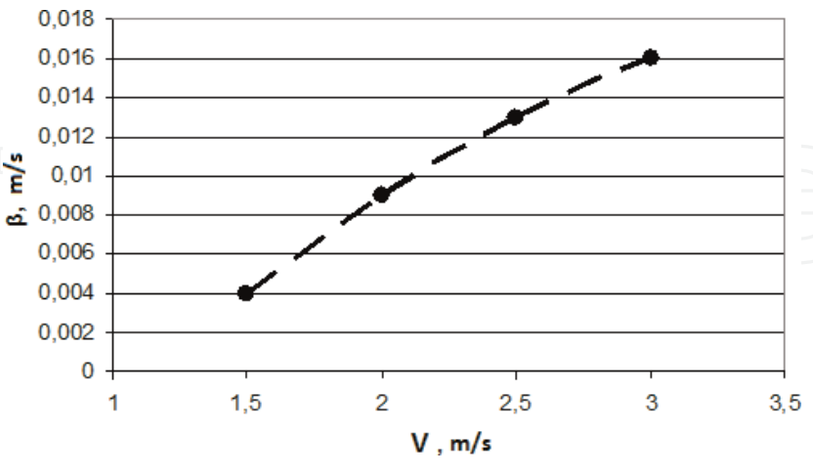


Figure 8.
Dependence of the mass transfer coefficient on the drying agent's motion velocity.

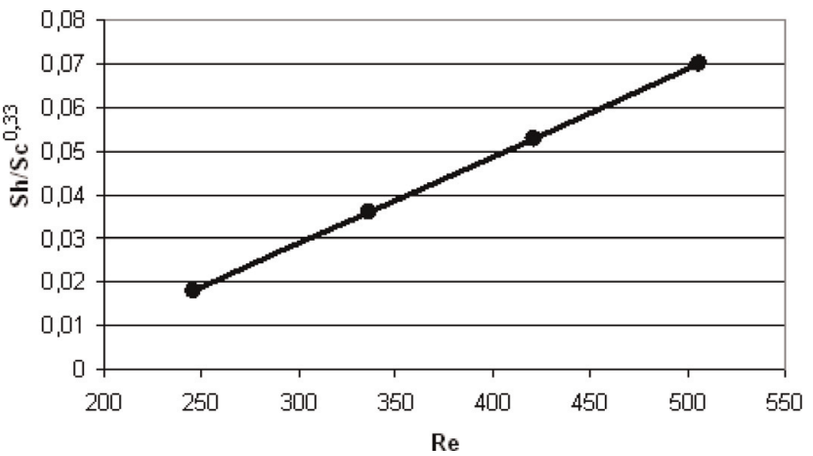


Figure 9.
Graphical dependency $Sh/Sc^{0.33} = f(Re)$ to define the coefficient A_1 and equation stage m.

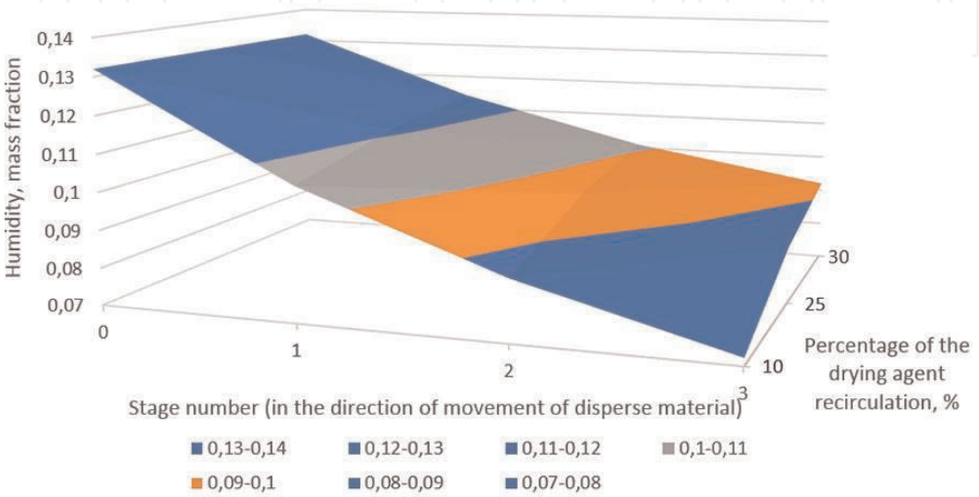


Figure 10.
Influence of the drying agent recirculation method on the change of the moisture content in the disperse material.

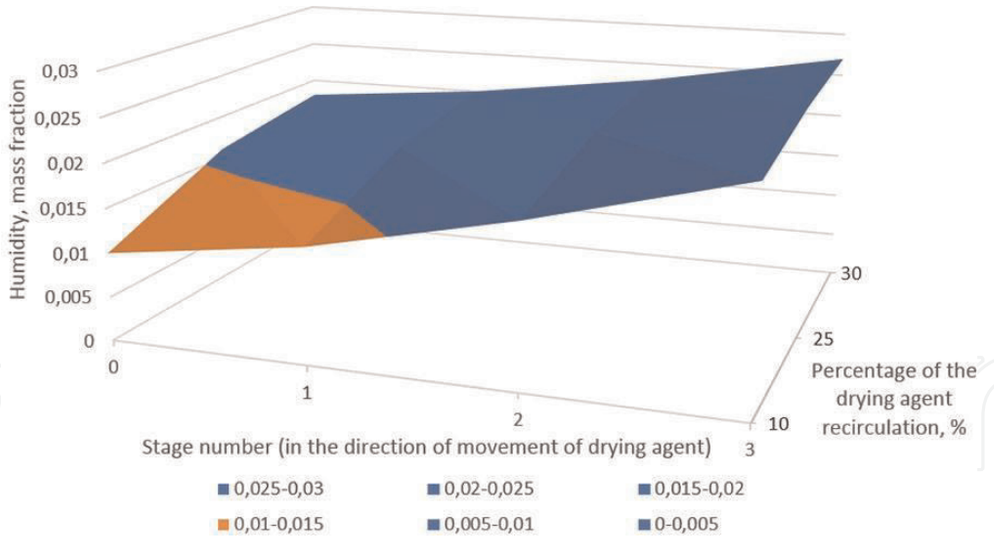


Figure 11.
Influence of the drying agent recirculation method on the change of the moisture content in the drying agent.

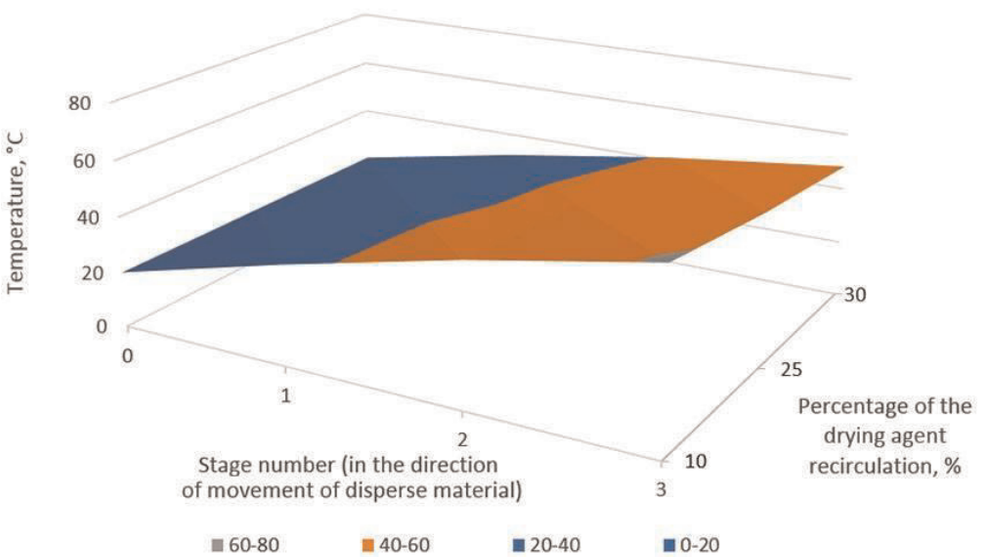


Figure 12.
Influence of the drying agent recirculation method on the temperature change of the disperse material.

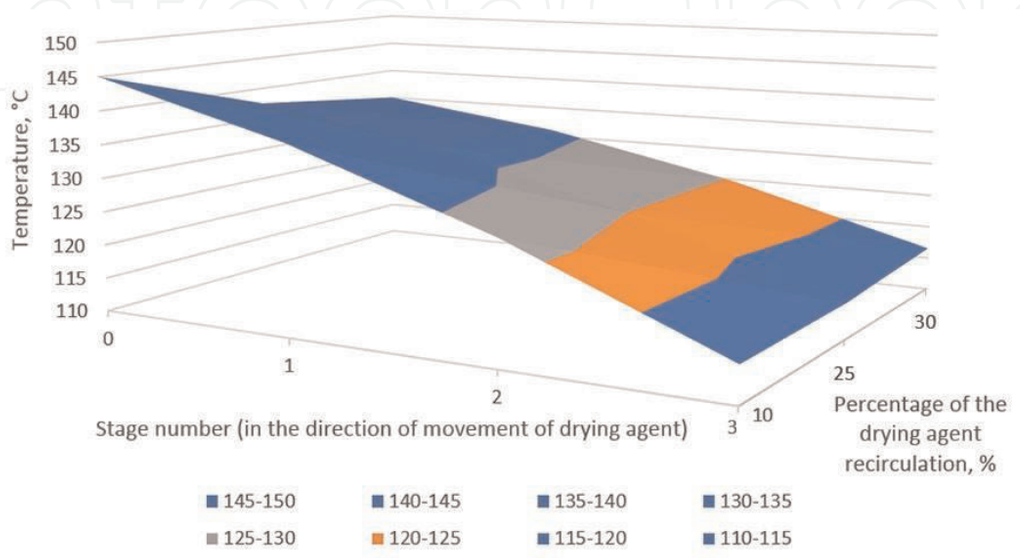


Figure 13.
An influence of the drying agent recirculation method on the temperature change of the drying agent.

The graphical dependency from Eq. (17) shows (**Figure 9**) that coefficient A_1 = 0.008, m = 0.47. The coefficient n is 0.33 for the situation when the drying agent's parameters were slightly changed during the experiment [8].

Taking into account the obtained values of the coefficient A_1 and equation stage m, the criterial value (18) will be as follows:

$$Sh = 0.008 \cdot Sc^{0.33} \cdot \mathrm{Re}^{0.47}. \tag{19}$$

3.3 Kinetics and drying efficiency

The organization of the drying agent's motion may have a considerable influence on the quality indicators of the dried material and the properties of the drying

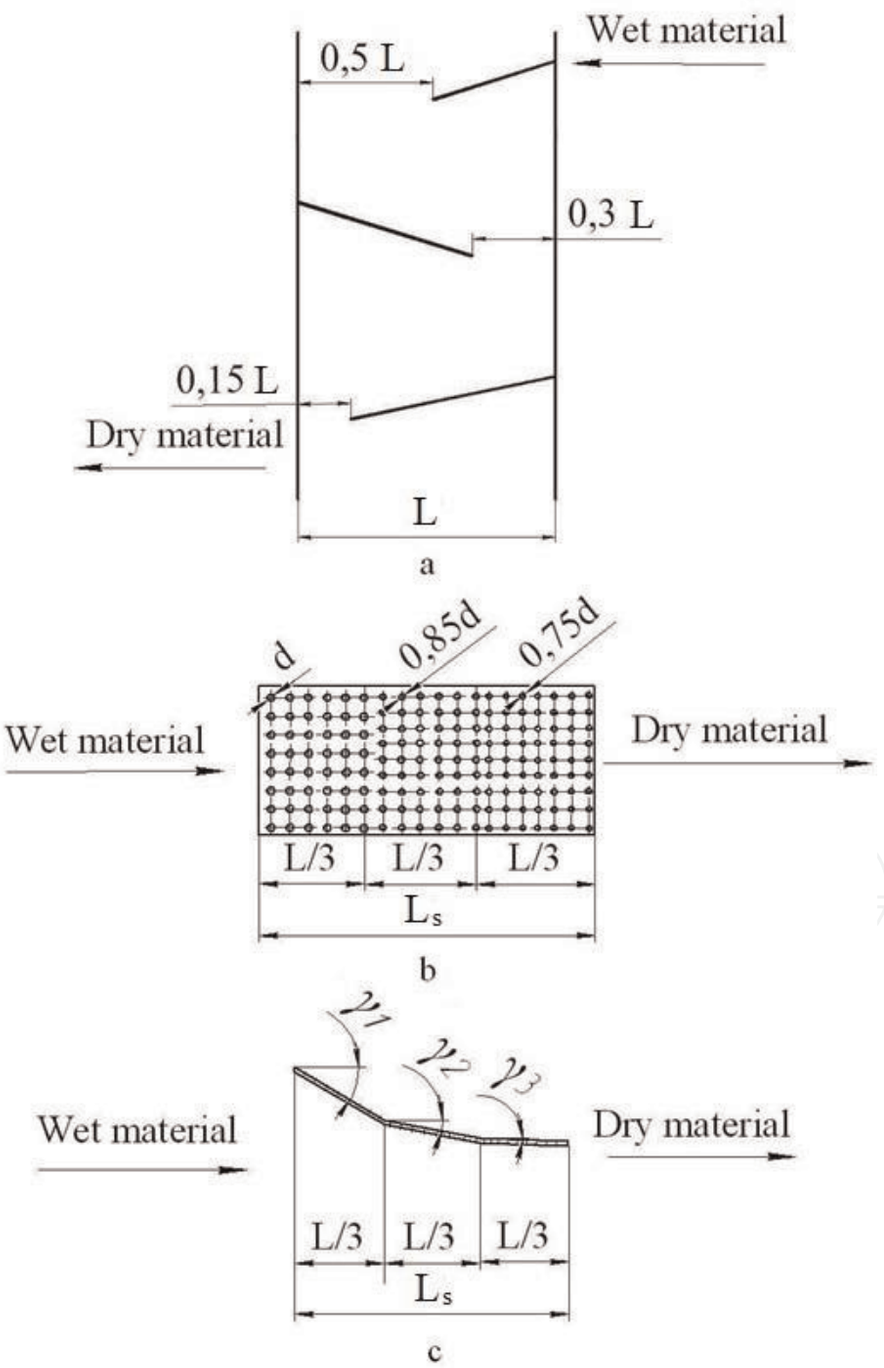


Figure 14.
Constructions of shelves in the multistage gravitational shelf dryer [13–15]: (a) shelf with a different gap on the height of dryer, (b) sectioned shelf with variable perforation of sections, and (c) partitioned sections shelf with constant perforation and variable angle of inclination.

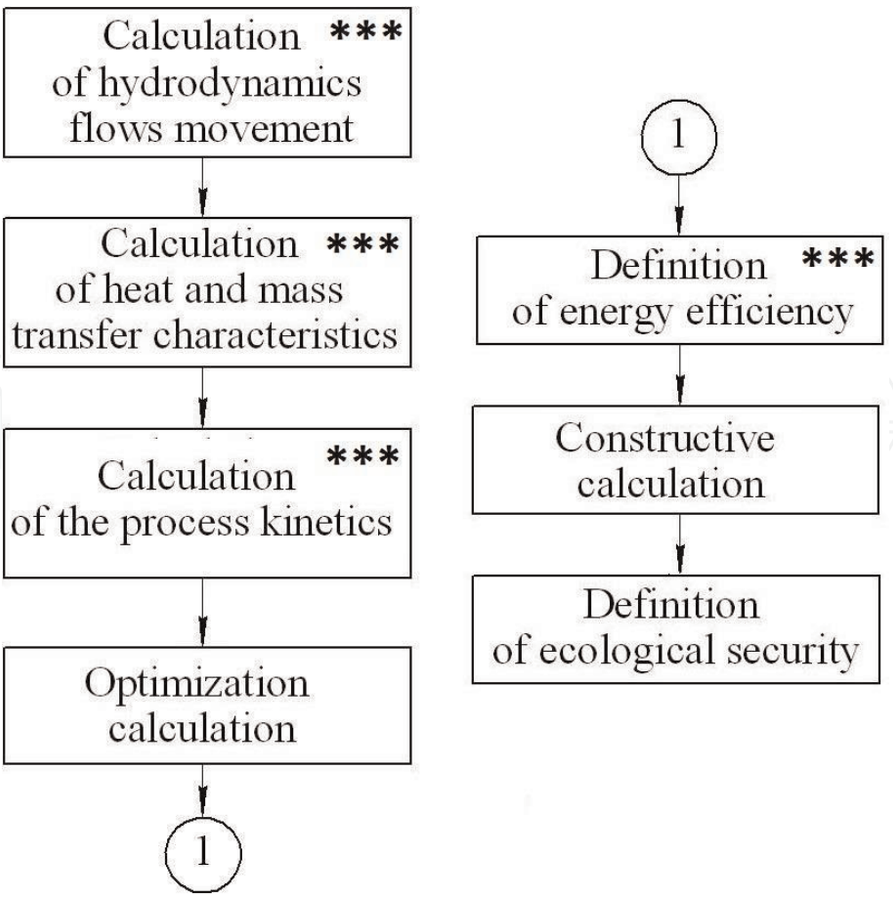


Figure 15.
*Block scheme of the algorithm to calculate the multistage gravitational shelf dryer (symbol *** shows the blocks which are described in this work).*

agent. That has evolved several studies, the results of which are presented in **Figures 10–13**. Their analysis enables us to select the method to organize the drying agent's motion, which consumes the least energy and ensures the necessary complete removal of moisture from the disperse material.

The analysis of the figures shows that the features of the dispersed material and the drying agent are changed according to one law; each of the technological indicators in the drying agent differently influences the intensity of the increase or decrease of parameters. The figures show that there is no function extremum on the graphical dependencies, which is explained by the regularities of the convective drying kinetics—the parameters' change of the contacting flows in each of the periods occurs monotonically with different intensity on separate sites depending on the dehydration conditions.

Different constructions of the shelves (**Figure 14**) enable us to control the residence time of the dispersed phase in the dryer's workspace.

Block scheme of the algorithm to calculate the multistage gravitational shelf dryer is represented in **Figure 15**.

4. Experimental research and practical implementation

During the optimization calculations, the necessity to obtain certain empiric dependencies has been revealed. They would identify some quantities, especially important for the shelf dryer's design development.

The experimental investigations were carried out on a shelf dryer model, the design parameters of which corresponded to the picture in **Figure 1**. Experiments to

study the properties of the two-phase flow hydrodynamics in a shelf device were carried out at gas flow velocity of 1–5 m/s, specific capacity on the source material 6–10 kg/(m^2 s).

At low gas flow velocities of 0.5–1 m/s, particles of the material move along the surface of the sloping shelf at a velocity of 0.2–0.3 m/s in the form of a rapidly "skipping" layer. The particles of the material are braked at the wall of the device in the discharge space and are accumulated on the surface of the wall (**Figure 16a**) after moving over the surface of the shelf. This accumulated layer is blown by a gas jet, which is formed by a discharge gap between the lower end of the shelf and the wall of the device. As the gas flow velocity increases to 2.5–4 m/s, the porosity of the layer decreases to 0.75–0.8, and the concentration of particles in the layer increases to 40–50 kg/m^2 s.

Small particles, in which the inertia force during their discharge from the surface of the sloping shelf is insufficient to overcome the kinetic energy of the gas jet, are picked up by the jet and move along a curved path to the upper part of the device—the separation zone. On the photo (**Figure 16a**), it is seen by the distinct tracks of the trajectory. Large particles, overcoming the aerodynamic drag of the gas jet, fall out of the layer through the discharge space down. The described hydrodynamic regime is called "gravitationally falling layer." This mode is implemented on the shelves, installed with a width of the discharge gap (0.3–0.5) L and a free area of 5–10%. Therefore, the maximum efficiency of small fraction ablation by the gas flow is achieved (**Figure 17**). The velocity of the complete ablation of the small fraction without large particles in it—the second critical velocity—is as follows:

$$Re_{2cr} = 0.1Ar^{0.7}, \text{ with } Ar \leq 62,000, \tag{20}$$

$$V_{cr} = \frac{\mathrm{Re}_{2cr} \cdot \nu}{d_{gre}} \tag{21}$$

where Ar is the Archimedes criterion, $Ar = \frac{d_{gre}^3 \cdot (\rho_{gr} - \rho_g) \cdot g}{\nu^2 \cdot \rho_g}$.

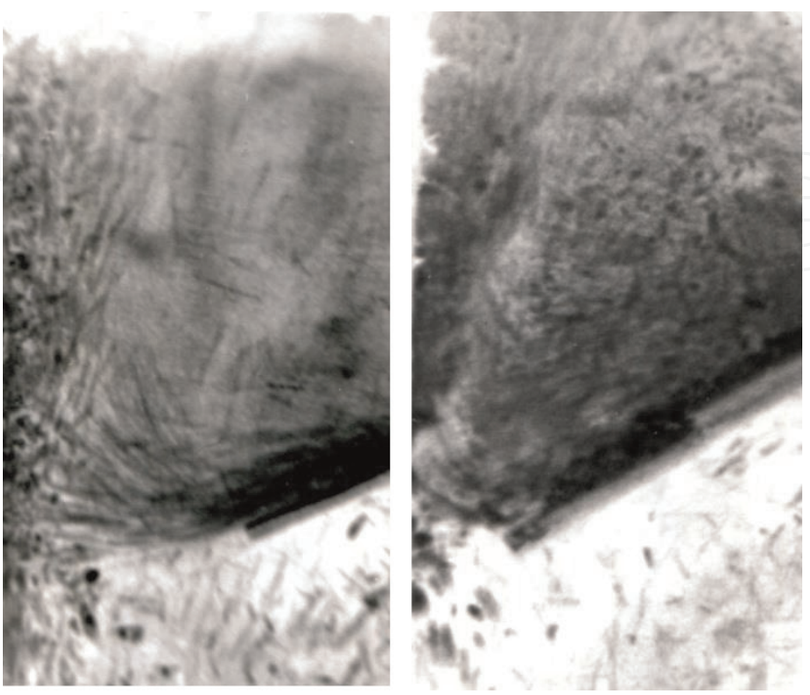


Figure 16.
The photo of the hydrodynamic modes of the shelf dryer: (a) "gravitationally falling layer" regime and (b) "weighted layer" regime.

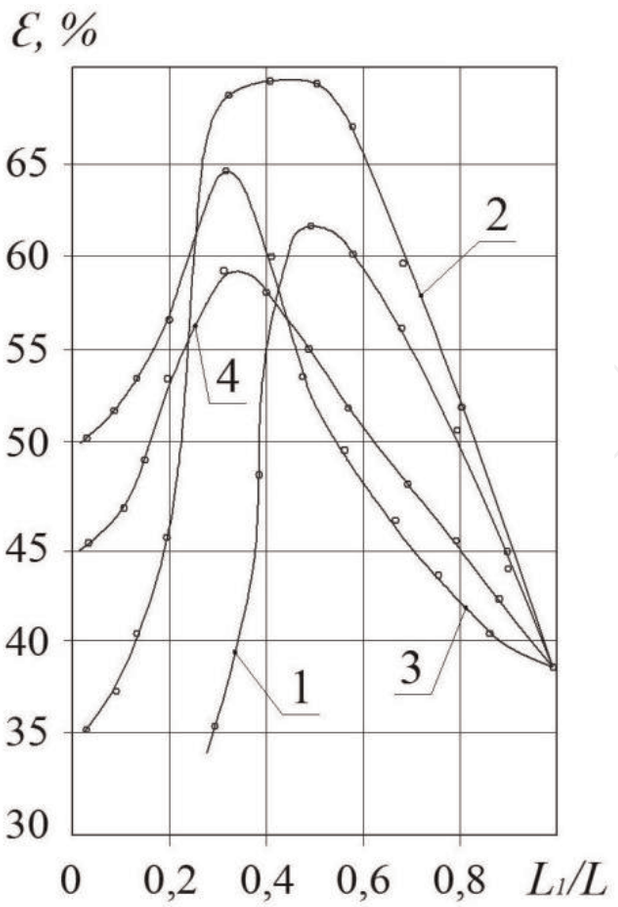


Figure 17.
The influence of the design (constructive) parameters of the shelf on the extraction efficiency of the fraction less than 1 mm. The free area of the shelf: 1–4, respectively, 0, 5, 15, and 30%. The tilt angle of the shelf is 30°. Material is a polydisperse mixture of the granular superphosphate.

Reducing the width of the discharge space up to (0.15–0.2) L and increasing the free area of the shelf up to 15%, owing to the growing kinetic energy of the gas jet, the continuously circulating vortex layer of particles above the sloping shelf surface is formed (**Figure 16b**). Therefore, the particles of the material are moving on the surface of the sloping shelf in the form of the tightened (compressed) layer at the velocity of 0.05–0.15 m/s, and in the area above, the discharge space—in the form of weighted, intensively circulating layer. The porosity of this layer is 0.65–0.7 (coincides with fluidized systems' porosity), and concentration of the particles in the workspace of the device is 160–280 kg/m^3. The described hydrodynamic regime is called the "weighted layer." The velocity at which the "weighted layer" mode is implemented—the critical velocity when the weighting is started is calculated as follows:

$$R_{wl} = Re_w \cdot k \cdot (L1/L), k = 1.19 \cdot \ lg\ (100 \cdot f_a) + 0.005, \tag{22}$$

$$V_{wl} = \frac{\mathrm{Re}_{wl} \cdot \nu}{d_{gre}}, \tag{23}$$

where Re_w is the Reynolds criterion for particle staying in the gas flow, $\mathrm{Re}_w = \frac{V_w \cdot d_{gre}}{\nu}$; V_w is the velocity of the medium-size particle hovering; f_a is the free area of the shelf (%).

The effect of the gas flow velocity on the intensity of the interphase heat transfer process is represented by the dependence of the Nusselt criterion on the Reynolds

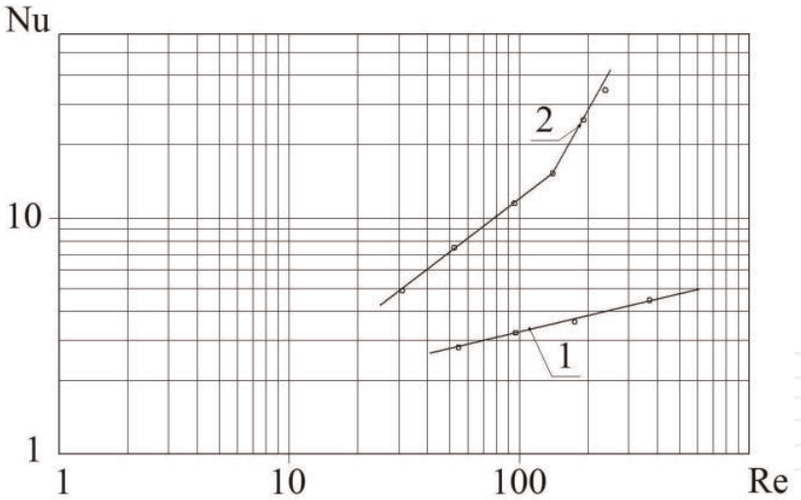


Figure 18.
Influence of the gas flow velocity on the interphase heat transfer intensity: (1) "gravitationally falling layer" mode, shelf parameters: $L_1/L = 0.5$; $f_a = 5\%$; (2) "weighted layer" mode, shelf parameters: $L_1/L = 0.15$; $f_a = 15\%$.

criterion—Nu = f (Re) (**Figure 18**). These dependencies are described with the following criteria equations:

$$\text{"gravitationally falling layer mode"} Nu = 1.5 \cdot Re^{0.21}, \tag{24}$$

$$\text{"weighted layer"mode } Nu = 0.38 \cdot Re^{0.73}. \tag{25}$$

Equations (24) and (25) are valid for $0 \leq \text{Re} \leq 500$.

The above dependencies in the "weighted layer" mode show that the values of the Nusselt criterion are significantly higher than values, which are peculiar for the "gravitationally falling layer" mode. The sufficiently high intensity of heat and mass transfer processes in the "weighted layer" mode is explained by the fact that in this mode the gas jet entering the weighted layer through the discharge gap at sufficiently high velocity has the greatest intensifying effect. Measures of the single-phase flow velocity, carried out by a thermal anemometer in the intersection above the shelf, showed that at gas jet velocities in the discharge space of 6–12 m/s, local heat transfer coefficients at the site of material particles contact with the gas jet are 400–500 W/(m^2 K). These values are peculiar for the intensive heat transfer conditions in the core of the spouting layer and exceed the average heat transfer coefficients for fluidized beds (100–400 W/(m^2 K)) and the pneumatic transportation mode (100–200 W/(m^2 K)).

The rapid evaporation of moisture in the zone above the discharge space leads to some temperature drop of the hot gas before it contacts with the main layer of particles, weighted above the shelf. Experimental studies show that the heating temperature of particles in the zone of contact with the gas jet entering the discharge gap is 1.5–2.0 times higher than that in a weighted layer on the surface of the shelf. It uses a drying agent with higher inlet temperature (1.5–1.8 times higher than melting temperature) than it is acceptable for dryers of the fluidized bed, without fear of the thermal damage of particles.

The investigated construction of the shelf dryer was tested when drying the fine- and coarse-crystalline potassium chloride, sodium pyrosulfite, iron, and nickel powders (**Table 1**).

The shelf dryer, where experimental tests were carried out, is a vertical rectangular-sectioned shaft, inside which the sloping perforated shelves are located in cascade on opposite sides (**Figure 1**). Wet material is fed by the batcher to the

Material	The velocity of the drying agent, m/s	Humidity, % wt			Moisture removal intensity, kg/(m^3 h)
		Source material	Undershooting	Ablation	
Fine-coarse potassium chloride:					
	1.32	6.1	0.35	0.24	421
Coarse-crystalline	1.5	6.1	0.1	0.06	462
	1.45	8.0	1.2	0.2	1025
	1.9	7.0	0.1	0.17	527
	2.1	8.0	0.11	0.1	1173
	2.3	7.0	0.14	0.1	528
Sodium pyrosulfite	2.8	5.0	0.5	0.1	250
	3.3	5.0	0.5	0.1	346
	3.5	6.0	0.6	0.2	258
Iron powder	2.0	10.0	0.34	0.3	1826
Nickel powder	2.3	11.3	0.4	0.3	600

Table 1.
Results of the drying of the granular materials in the shelf dryer.

upper shelf, is weighed above it, and is divided into small and large fractions. The upper shelf works in the hydrodynamic regime of the "gravitationally falling layer." In this mode, the dedusting process of materials, i.e., the removal of small particles from the initial mixture by the minimum interface, is effectively carried out. The minimum interface for shelf devices is 50–70 μm. The small particles are carried away by the drying gas agent into the separation space and then captured by a cyclone in which they are dried. Large particles fall down through the discharge space to the lower shelf.

When drying the materials, which are prone to the formation of lumps and strongly sticking to surfaces, the distance from the delivery point of the wet product into the device to the upper shelf has to be at least 0.3–0.5 m. The material, passing this distance, breaks up into small pieces and is partially dried. A hydrodynamic regime of the "weighted layer" is created on the lower shelf, in which, due to the intensive circulation and mixing of particles in the layer, the drying process is effectively carried out. The longer residence time of the particles in this layer also contributes to it.

The wet material, discharged from the upper shelf, enters the lower shelf from the top of the weighted layer, is drawn into the circulation, and is dried quickly. The share of the dried material falls through the discharge space into the hopper, in which a large fraction of the dried product is collected.

Thanks to the shelf contact elements, shown by the data of **Table 1**, the drying process takes place at the drying agent's moderate velocities (maximum 3.5 m/s) and at a large moisture intensity of the dryer's workspace which is up to 1000–1500 kg/(m^3 h). Due to the intensive contact between phases in the shelve devices, the drying process is carried out at high specific loads of up to 15–20 kg/(m^2 s), significantly exceeding the specific loads of 0.1–1.5 kg/(m^2 s) for fluidized bed devices. The specific consumption of the drying agent in the shelf dryers reaches

0.5–0.7 m^3/kg, and the hydraulic resistance is 1300–1500 Pa, respectively, against the values of 1.4–2.8 m^3/kg and 1800–2200 Pa for fluidized bed devices. The working path of the pneumatic pipe dryer, in which energy is expended to accelerate and to lift the drying material, has a hydraulic resistance of 1600–2000 Pa.

An additional advantage of shelf dryers is the simultaneous dedusting of the drying material. Fine-crystalline potassium chloride, containing 7–10% of the small fraction with a particle size of less than 100 μm in the initial mixture, after processing in a shelf device at a gas flow velocity of 1.4–1.5 m/s, had 1.2–5.5% of the small fraction in the final product (undershooting) and 60–80% of the small fraction in ablation. Coarse-crystalline potassium chloride, containing 4–10% of the small fraction with a particle size of less than 100 μm in the initial mixture, had 2–5% of the small fraction in the final product (undershooting) at a gas flow velocity of 1.3–1.4 m/s and 58–65% of the small fraction in the ablation. The extraction degree of the small fraction into the ablation was 70–90%. When the gas flow velocity exceeds 1.5 m/s in the final product, the small fraction is practically absent, and the content of the coarse fraction (more than 100 μm) in ablation is 3–5%.

The small fraction was completely extracted from the polydisperse mixture of granulated superphosphate containing up to 20% of the small fraction with particle sizes less than 1 mm, after processing in the shelf device at a gas flow velocity of 3.5–3.8 m/s, into the ablation. Therefore, the extraction degree of the small fraction into ablation was 80–85%.

In order to prevent the coarse fraction ablation by the gas flow and increasing the residence time of particles in the separation space for drying the ablative fractions, the upper section with a constant intersection was replaced with a conical free intersection [16] or with shelf contact elements [17].

Thus, the shelf dryers achieve the higher technological effect than typical constructions of the fluidized bed dryers and pneumatic pipe dryers, with less energy, capital costs, and sizes.

5. Conclusions

The convective shelf dryer construction with active aerodynamic processing modes is proposed. The developed engineering method for the shelf dryer calculation made it possible to define the constructive parameters of the device, ensuring the minimum required drying time of the wet material in the device to a predetermined humidity index. The demonstrated author's program Multistage Fluidizer® for computer implementation of the engineering calculation method made it possible to optimize the constructive and operating parameters of the drying process in the shelf device. It was shown that a shelf dryer should have, for example, three shelf contacts with various widths of the discharge space and various free areas of the shelves.

The author shows various hydrodynamic regimes to weigh particles of a material by a gas flow, depending on the constructive parameters of shelf contacts.

The effectiveness of the shelf device to carry out the drying and dedusting processes of granular and powder materials simultaneously was experimentally proven.

Acknowledgements

This research work has been supported by the Slovak Grant Agency VEGA Grant No. 1/0731/16 "Development of Modern Numerical and Experimental

Methods of Mechanical System Analysis," by Cultural and Educational Grant Agency of the Slovak Republic (KEGA) Project No. KEGA 002TnUAD-4/2019, and by the Ministry of Science and Education of Ukraine under the project "Small-scale energy-saving modules with the use of multifunctional devices with intensive hydrodynamics for the production, modification and encapsulation of granules," Project No. 0119U100834.

Conflict of interest

The authors declare that they have no competing interests.

Author details

Artem Artyukhov[1*], Nadiia Artyukhova[1], Ruslan Ostroha[1], Mykola Yukhymenko[1], Jozef Bocko[2] and Jan Krmela[3,4]

1 Sumy State University, Sumy, Ukraine

2 Technical University of Košice, Košice, Slovak Republic

3 Alexander Dubcek University of Trencin, Puchov, Slovak Republic

4 University of Pardubice, Pardubice, Czech Republic

*Address all correspondence to: a.artyukhov@pohnp.sumdu.edu.ua

IntechOpen

© 2019 The Author(s). Licensee IntechOpen. This chapter is distributed under the terms of the Creative Commons Attribution License (http://creativecommons.org/licenses/by/3.0), which permits unrestricted use, distribution, and reproduction in any medium, provided the original work is properly cited. CC BY

References

[1] Delgado JMPQ, Barbosa de Lima AG, editors. Transport Phenomena and Drying of Solids and Particulate Materials. Switzerland: Springer International Publishing; 2014. 115p

[2] Kowalski SJ, editor. Drying of Porous Materials. Netherlands: Springer; 2007. 231p

[3] Sazhin BS, Sazhin VB. Scientific Principles of Drying Technology. USA: Begell House Publishers Inc.; 2007. 509p

[4] Kowalski SJ. Thermomechanics of Drying Processes. Germany: Springer-Verlag Berlin Heidelberg; 2003. 358p

[5] Delagado JMPQ, Barbosa de Lima AG, editors. Drying and Energy Technologies. Switzerland: Springer International Publishing; 2016. 228p

[6] Mujumdar AS, editor. Handbook of Industrial Drying. 4th ed. USA: CRC Press Taylor & Francis Group; 2014. 1348p

[7] Law CL, Azharul K, editors. Intermittent and Nonstationary Drying Technologies: Principles and Applications. 1st ed. USA: CRC Press Taylor & Francis Group; 2017. 244p

[8] Artyukhova NA, Shandyba AB, Artyukhov AE. Energy efficiency assessment of multi-stage convective drying of concentrates and mineral raw materials. Naukovyi Visnyk Natsionalnoho Hirnychoho Universytetu. 2014;**1**:92-98

[9] Artyukhov AE, Sklabinskyi VI. Experimental and industrial implementation of porous ammonium nitrate producing process in vortex granulators. Naukovyi Visnyk Natsionalnoho Hirnychoho Universytetu. 2013;**6**:42-48

[10] Kudra T, Mujumdar AS. Advanced Drying Technologies. 2nd ed. USA: CRC Press; 2009. 438p

[11] Artyukhova NA. Multistage finish drying of the N_4HNO_3 porous granules as a factor for nanoporous structure quality improvement. Journal of Nano- and Electronic Physics. 2018;**10**(3): 03030-1-03030-5

[12] Artyukhov AE, Artyukhova NO, Obodyak VK, Horishnyak AO. Certificate of authorship No. 79141 (Ukraine). Computer program Multistage Fluidizer©

[13] Artyukhova NO, Yukhymenko MP, Artyukhov AE, Shandyba AB. Patent No. 74070, (Ukraine). Device for drying of disperse materials

[14] Artyukhova NO, Yukhymenko MP, Artyukhov AE, Shandyba AB. Patent No. 81720, (Ukraine). Device for drying of disperse materials

[15] Artyukhov AE, Artyukhova NO, Shandyba AB. Patent No. 92423, (Ukraine). Device for drying of disperse materials

[16] Yukhymenko M, Ostroha R, Litvinenko A, Bocko J. Estimation of gas flow dustiness in the main pipelines of booster compressor stations. IOP Conference Series: Materials Science and Engineering. 2017;**233**:012026

[17] Lytvynenko A, Yukhymenko M, Pavlenko I, Pitel J, Mizakova J, Lytvynenko O, et al. Ensuring the reliability of pneumatic classification process for granular material in a rhomb-shaped apparatus. Applied Sciences. 2019;**9**:1604